

MESA - STATUS OF THE IMPLEMENTATION OF THE MicroTCA.4-BASED LLRF CONTROL SYSTEM

J. Bai*, K. Aulenbacher, F. Fichtner, R. Heine, J. Diefenbach

Institut für Kernphysik, Johannes Gutenberg-Universität Mainz, D-55099 Mainz, Germany

Abstract

The Mainz Energy-recovering Superconducting Accelerator (MESA) at the Institut für Kernphysik (KPH) at Johannes Gutenberg-Universität Mainz is a multi-turn Energy-Recovery-Linac (ERL), aiming to serve as user facility for particle physics experiments. The RF-accelerating systems of MESA consist of 12 cavities, four of them are 9-cell TESLA superconducting (SC) cavities. They operate in continuous wave (CW) mode. In order to control the radio frequency (RF) amplitude and phase within the 12 cavities with the required accuracy and stability better than 0.01% and 0.01°, the Micro Telecommunications Computing Architecture (MicroTCA.4) based digital low-level RF (LLRF) control system based on the development at DESY, Hamburg will be adapted for the MESA cavities. A Matlab/Simulink model was created to find the proper control parameters and to predict the system performance. In this paper, the simulation results, the progress of the implementation and the first tests of the LLRF system for MESA are presented.

INTRODUCTION

The MESA accelerator is a multi-turn ERL working at low energy and CW mode for particle physics experiments, which is currently under construction at KPH, Johannes Gutenberg-Universität Mainz. MESA has two different operation modes, the external beam (EB) mode and the energy recovery (ER) mode, which serve for two physics-experiments. The EB mode is mainly to measure the weak mixing angle with the highest accuracy. The polarized electron beam of 150 μA current at 155 MeV energy is dumped after being used with the external fixed target experiment P2. In the ER mode, MESA runs as an ERL, generating an unpolarised beam of 1 mA at 105 MeV. An internal fixed target experiment named MAGIX (MESA Gas Internal target eXperiment) is used in this mode. After a further upgrade of the cryomodules, MESA can achieve a beam current of 10 mA in the ER mode.

MESA CAVITIES

The MESA RF system topology includes four 9-cell TESLA SC cavities working at 1.3 GHz, four normal conducting (NC) pre-accelerator cavities at 1.3 GHz, two chopper cavities at 1.3 GHz, one buncher cavity at 1.3 GHz and the second buncher cavity at 2.6 GHz, which are illustrated in Fig. 1. All cavities will be driven by their own solid state power amplifier (SSPA). Due to the narrow bandwidth of 100 Hz, the SC cavity has tighter requirements for the am-

plitude and phase stability of the electrical field within the cavities. Tab. 1 shows the main parameters of the MESA SC cavity [1]. MESA requires an amplitude and phase stability better than 0.01% and 0.01°.

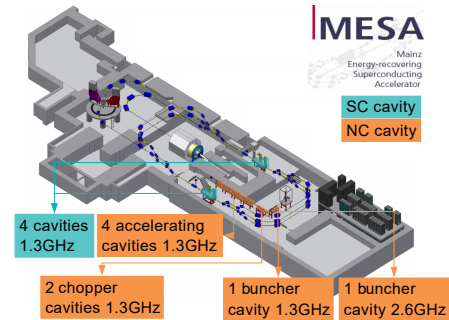


Figure 1: Overview of MESA RF system topology.

Table 1: Main Parameters of the MESA SC Cavity

Max E_{acc}	RF power	Q_L	Bandwidth
12.5 MV/cavity	15 kW	1.4×10^7	100 Hz

LLRF SYSTEM

MESA makes use of the MicroTCA.4 based LLRF system mainly developed by DESY [2]. All cavities are fed by their own RF power source, therefore we are implementing a single cavity LLRF control system [3]. The combination of a SIS8300-L Advanced Mezzanine Card (AMC) digitizer and a DWC8VM1 Rear Transition Module (RTM) analog boards purchased from Struck [4] offers a very compact solution for the single cavity control. The DWC8VM1 consists of 8 channel high frequency down-converters and one channel high frequency up-converter, which is the so-called vector modulator (VM) [5]. In the MESA project, the 1.3 GHz RF input signal picked up by the antenna will be down-converted to a 54 MHz intermediate frequency (IF) signal by means of a 1.354 GHz local oscillator (LO) signal and a low pass filter. The central components of the SIS8300-L are 10 125 MS/s 16-bit analog-digital converters (ADC), a Xilinx Virtex 6 FPGA and two 250 MS/s 16-bit digital-analog converters (DAC) [6]. The polar representation of an RF signal can be decomposed into its Cartesian representation by the so-called inphase (I) and quadrature (Q) components [7]. The advantage of this procedure is that phase and amplitude can be controlled simultaneously using setpoint values in I/Q description. The IF signal is sampled at the 81 MHz by ADCs. On the FPGA, the control deviation is calculated from the

* jibai@uni-mainz.de

Content from this work may be used under the terms of the CC BY 3.0 licence (© 2018). Any distribution of this work must maintain attribution to the author(s), title of the work, publisher, and DOI.

I/Q components measured by the ADCs and the setpoints given by the central control system. The control of the cavity amplitude and phase within specified requirements are accomplished by two PI (proportional-integral) controllers [8]. The VM is controlled by the I/Q component output signals and generates the RF driving signal for the SSPA based on the 1.3 GHz reference input (REF) signal.

Apart from the phase and amplitude control, the LLRF system is also responsible for the frequency detuning control of the SC cavity. This paper concentrates only on the phase and amplitude control.

LLRF TEST SETUP

The first test setup including of a phase shifter was built to simulate the cavity pick-up signals for the LLRF. Figure 2 is the block diagram of the test setup. The 81 MHz ADC sampling clock, the 1.354 GHz LO signal and the 1.3 GHz REF signal are generated by the synchronization system, which is composed of three synchronized signal generators (a Hewlett Packard 83732B signal generator at 20 dBm in 81 MHz, a Agilent E4432B ESG-D series signal generator at 16 dBm in 1.381 GHz and a Hewlett Packard E4432B ESG-D series signal generator at 16 dBm) in 54 MHz, mixers, filters, amplifiers and power dividers. The 1.3 GHz RF signal is distributed into three paths. One is used as the VM REF signal. Another is the RF input signal of a down converter and a L3 Narda-ATM 360°/GHz phase shifter series P1103D¹ is located in between. An Agilent Technologies MSO9254A mixed signal oscilloscope is used to observe the output reference signal and the VM output signal. As expected the phase difference between the VM output signal and the output reference signal varies when the P1103D shifts phase of the RF input signal. Figure 3 shows the front side view of the test setup.

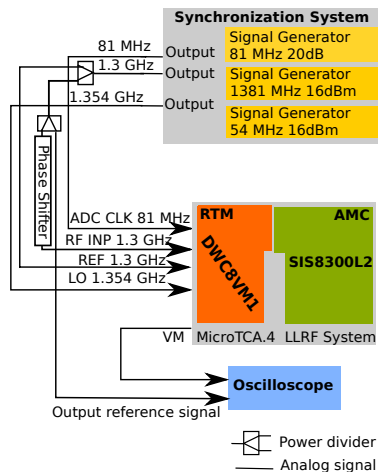


Figure 2: Block diagram of the LLRF test setup.

The RF input signal goes through both the analog and digital processes, which are illustrated in Fig. 4. A detailed

¹ <https://www.atmmicrowave.com/coaxial/phase-shifter-line-stretcher/>



Figure 3: Front side view of the LLRF test setup.

description of the individual processing steps can be found in [9]. In order to maintain the adequate amplitude stability it is necessary to calibrate the DAC offset and gain errors. Then the amplitude stability achieves $\pm 3.5\%$ instead of 16% without the calibration. The PI controller will guarantee the phase and amplitude stability requirements. Figure 5 shows the time difference between the VM output signal and the output reference signal under a certain phase shift.

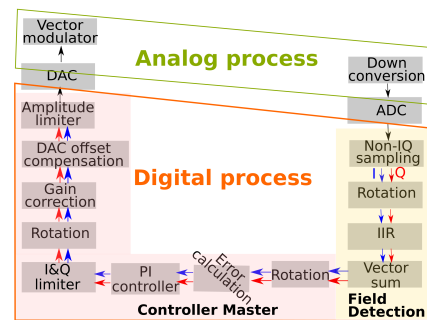


Figure 4: Block diagram of the LLRF firmware.

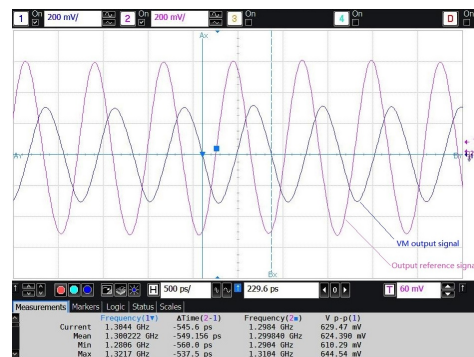


Figure 5: VM output and reference signal and their phase difference observed by the oscilloscope.

MODEL SIMULATION

A Matlab/Simulink model was developed to simulate the system response, perform the stability analysis of the con-

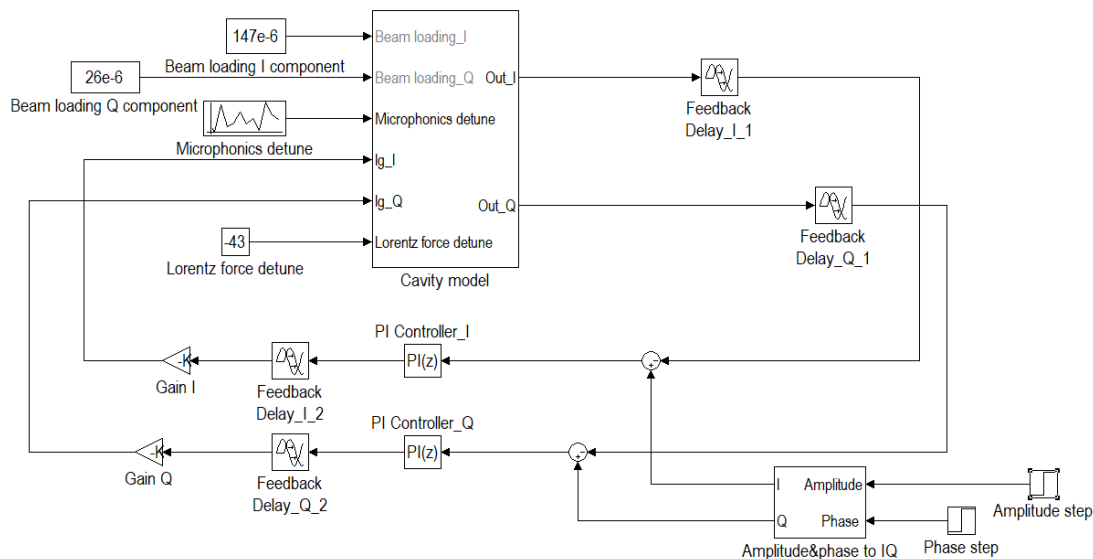


Figure 6: Simulink model of the LLRF control system.

control system and optimize control parameters. The amplitude and phase control model is shown in Fig. 6. The non-linear dynamics of a single RF cavity can be represented by a state-space equation [10]. Two PI controllers are individually used for I/Q component control. In this paper the EB mode is taken as an example, the amplitude and phase step response were obtained to analyze the stability of the control system. The amplitude setpoint is 12.5 MV and the phase setpoint is 10°. The beam loading I/Q components are calculated for the beam current 150 μ A and the synchronous phase 10°. The Lorentz force detune of -43 Hz is estimated by $\Delta f = -k \cdot E_{acc}^2$, where Δf is the frequency shift, k the Lorentz force coefficient and E_{acc} the accelerating gradient [11]. The microphonics detune is assumed to be a uniform distribution between -50 Hz and 50 Hz. Figure 7 shows the amplitude and phase step responses.

The simulation proved that the I/Q component closed-loops are stable and the cavity field amplitude and phase stability are better than 0.01% and 0.01° after 500 μ s. For the practical application, the dead time of the simulation must be corrected according to the LLRF system.

CONCLUSION & OUTLOOK

In summary, as the first functional test, the open-loop phase shift of the MicroTCA.4 based LLRF system was tested. The phase of the VM output signal shifts according to the phase shift of the RF input signal. During this process the amplitude stability reaches $\pm 3.5\%$ with the calibrated VM in the open-loop mode. The Matlab/Simulink model of the LLRF control system was developed to find the P and I gains for the PI controllers. In the coming months, in-depth analysis and tests will be done to assure that the system can fulfill all MESA requirements. The simulation will be used to find the optimum control parameters. Then the frequency detune control will be integrated into the system.

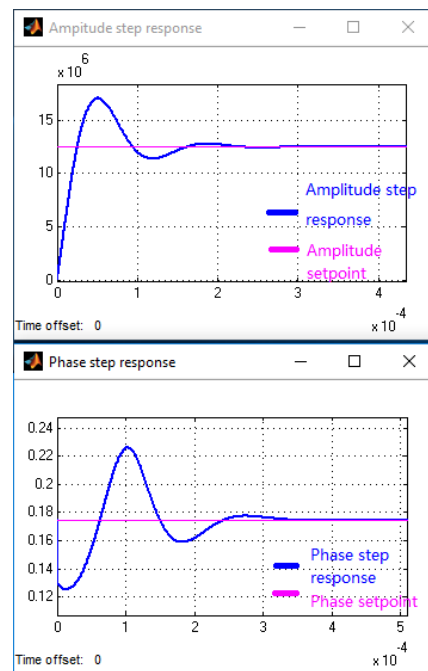


Figure 7: Amplitude and phase step responses of the LLRF control system model. Plot (top) is the amplitude step response with P gain = 400 and I gain = 25000000 and the plot (bottom) is the phase step response with P gain = 300 and I gain = 11000000.

ACKNOWLEDGEMENTS

Authors would like to thank the MicroTCA Technology Lab from DESY for providing the firmware of the MicroTCA.4 based LLRF control system. Further thanks to Pablo Echevarria Fernandez at HZB for his introduction to the firmware.

REFERENCES

- [1] R. Heine and F. Fichtner, "Concept of the High Power RF Systems for MESA," in *Proceedings, 8th International Particle Accelerator Conference (IPAC 2017), Copenhagen, Denmark, May 14-19, 2017*, pp. 4147–4149, JACOW, Geneva, Switzerland, 2017.
- [2] J. Branlard, G. Ayvazyan, V. Ayvazyan, M. Grecki, M. Hoffmann, T. Jeżyński, F. Ludwig, U. Mavrič, S. Pfeiffer, H. Schlarb, *et al.*, "MTCA. 4 LLRF System for the European XFEL," in *Proceedings, 20th International Conference "Mixed Design of Integrated Circuits and Systems"*, pp. 109–112, IEEE, 2013.
- [3] K. Przygoda, P. Echevarria, R. Rybaniec, H. Schlarb, and C. Schmidt, "MicroTCA.4 based Single Cavity Regulation including Piezo Controls," in *Proceedings, 7th International Particle Accelerator Conference (IPAC 2016): Busan, Korea, May 8-13, 2016*, p. THOAA03, 2016.
- [4] "Struck Innovative Systeme."
<http://www.struck.de/>.
- [5] "Datasheet of RTM-DWC8VM1."
https://techlab.desy.de/products/rtm/drtm_dwc8vm1/localfsExplorer_read?currentPath=/afs/desy.de/group/msk/www/html/TechLab/DRTM-DWC8VM1/Datasheet\%20DRTM-DWC8VM1.pdf.
- [6] "Datasheet of SIS8300-L2."
http://www.desy.de/~wwwuser/_publish/sis830012-m-x009-1-v101.pdf.
- [7] T. Schilcher, "Digital Signal Processing in RF Applications," *Digital Signal Processing CAS*, pp. 249–283, 2007.
- [8] K. J. Aström and T. Hägglund, *PID Controllers: Theory, Design, and Tuning*, vol. 2. Instrument society of America Research Triangle Park, NC, 1995.
- [9] I. Rutkowski, M. Hoffmann, H. Schlarb, L. Butkowski, and C. Schmidt, "Regae LLRF Control System Overview," in *Proceedings, 4th International Particle Accelerator Conference (IPAC 2013): Shanghai, China, May 12-17, 2013*, pp. 3210–3212, 2013.
- [10] M. Hernandez and W. Höfle, "Progress Report on SIMULINK Modelling of RF Cavity Control for SPL Extension to LINAC4," tech. rep., sLHC Project Report 0054, 2011.
- [11] Z. Li, C. Adolphsen, M. Ross, L. Xiao, T. Raubenheimer, O. Kononenko, and C. Rivetta, "Multi-physics Analysis of CW Superconducting Cavity for the LCLS-II Using ACE3P," in *Proceedings, 5th International Particle Accelerator Conference (IPAC 2014): Dresden, Germany, June 15-20, 2014*, pp. 2645–2647, 2014.